PROCEEDINGS OF SPIE

SPIEDigitalLibrary.org/conference-proceedings-of-spie

Ultrafast quantitative time-stretch imaging flow cytometry of phytoplankton

Queenie T. K. Lai, Andy K. S. Lau, Anson H. L. Tang, Kenneth K. Y. Wong, Kevin K. Tsia

Queenie T. K. Lai, Andy K. S. Lau, Anson H. L. Tang, Kenneth K. Y. Wong, Kevin K. Tsia, "Ultrafast quantitative time-stretch imaging flow cytometry of phytoplankton," Proc. SPIE 9720, High-Speed Biomedical Imaging and Spectroscopy: Toward Big Data Instrumentation and Management, 972011 (7 March 2016); doi: 10.1117/12.2212246

SPIE.

Event: SPIE BiOS, 2016, San Francisco, California, United States

Ultrafast quantitative time-stretch imaging flow cytometry of phytoplankton

Queenie T. K. Lai, Andy K. S. Lau, Anson H. L. Tang, Kenneth K. Y. Wong, and Kevin K. Tsia*

Department of Electrical and Electronic Engineering, The University of Hong Kong, Pokfulam Road, Hong Kong
*Corresponding author: tsia@hku.hk

ABSTRACT

Comprehensive quantification of phytoplankton abundance, sizes and other parameters, e.g. biomasses, has been an important, yet daunting task in aquatic sciences and biofuel research. It is primarily because of the lack of effective tool to image and thus accurately profile individual microalgae in a large population. The phytoplankton species are highly diversified and heterogeneous in terms of their sizes and the richness in morphological complexity. This fact makes time-stretch imaging, a new ultrafast real-time optical imaging technology, particularly suitable for ultralarge-scale taxonomic classification of phytoplankton together with quantitative image recognition and analysis. We here demonstrate quantitative imaging flow cytometry of single phytoplankton based on quantitative asymmetric-detection time-stretch optical microscopy (Q-ATOM) – a new time-stretch imaging modality for label-free quantitative phase imaging without interferometric implementations. Sharing the similar concept of Schlieren imaging, Q-ATOM accesses multiple phase-gradient contrasts of each single phytoplankton, from which the quantitative phase profile is computed. We employ such system to capture, at an imaging line-scan rate of 11.6 MHz, high-resolution images of two phytoplankton populations (scenedesmus and chlamydomonas) in ultrafast microfluidic flow (3 m/s). We further perform quantitative taxonomic screening analysis enabled by this technique. More importantly, the system can also generate quantitative phase images of single phytoplankton. This is especially useful for label-free quantification of biomasses (e.g. lipid droplets) of the particular species of interest – an important task adopted in biofuel applications. Combining machine learning for automated classification, Q-ATOM could be an attractive platform for continuous and real-time ultralarge-scale single-phytoplankton analysis.

Keywords: optical time-stretch, imaging flow cytometry, phytoplankton, quantitative phase imaging, asymmetric detection

1. INTRODUCTION

Phytoplankton (also called microalgae) as the foundation of carbon cycle and food ecosystem is indispensable in all aquatic systems such as lakes, ponds and sea, etc. The diversity of the species and growth of phytoplankton is closely related to the nutrients available in the environment and the carbon cycle. The relative abundance of each taxonomic group is an indicator of the environmental change in local (e.g. reservoir ecosystem and algal blooming) [1-3] and in global scale (e.g. global warming) [4,5]. As the phytoplankton species are greatly diversified, high throughput automated classification is developed [6,7] but is still limited by the frame rate of the CCD/CMOS sensor used in those instruments. By using optical time-stretch imaging flow cytometry [8–12], line scan rate of MHz could be achieved and "single-phytoplankton" analysis is demonstrated with classifying phytoplankton in [12]. Due to the interspecies and intraspecies heterogeneity and complexity of phytoplankton, single particle analysis which provide abundance, size, dry mass and cell volume information in a large scale will provide insights to ecosystem modeling and improve the classification between the dead, living, autotropic and heterotropic species which are not morphologically differentiable. The carbon, nitrogen and protein content could be estimated form the cell volume of the phytoplankton [13-15]. These parameters especially the carbon content could give deeper understanding to the carbon dynamics which directly affect the atmospheric CO_2 and earth's climate. Indeed, some types of phytoplankton contain rich useful substances such as lipids and carotene which can produce biofuel, other pharmaceutical and cosmetic products [16]. Comprehensive database and analytical methods on quantitative information of every single cell provide an attractive tool to better utilize the cultured species in biofuel, pharmaceutical and cosmetic production. Although one can determine the actual organic carbon content or other metabolite composition by biochemical method, there is no single tool to profile the phytoplankton individually and effectively. One of the most extensive methods to offer an accurate and comprehensive profile of each

High-Speed Biomedical Imaging and Spectroscopy: Toward Big Data Instrumentation and Management,
edited by Kevin K. Tsia, Keisuke Goda, Proc. of SPIE Vol. 9720, 972011 · © 2016 SPIE
CCC code: 1605-7422/16/$18 · doi: 10.1117/12.2212246

cell is by microscopic enumeration that calculates the volume by measuring a number of linear dimensions of the cell and assigning a simple geometrical model such as spherical, cylindrical and ellipsoidal [17,18]. Yet, this measurement is time-consuming, which requires an experienced expertise to examine the sample population and generate a certain discrepancy between the actual and estimated cell volume. Apart from manual inspection, electron particle counting is a more effective and rapid way but it measures bulk characteristics of all living organisms and non-living matters [17, 19]. Determination of pigment (e.g. chlorophyll *a*) concentration is another method of estimating cell volume but it is limited by volume of water and need complicated processes [17, 20]. Recently, estimation of cell volume by using imaging flow cytometry with the assumption of a simple geometrical model is developed with automated classification [21]. This is a higher through-put method but the biovolume can be miscalculated due to the existence of vacuoles, air bubbles in the phytoplankton cell. In the past decade, a series of quantitative phase imaging (QPI) techniques are developed, such as digital holographic microscopy [22], Hilbert phase microscopy [23] and synthetic phase microscopy [24]. These QPI techniques enable a label-free and accurate determination of the single cell dry mass and angular light scattering information [25] but they are not designated for ultra-large scale single-cell analysis, again, primarily due to the use of conventional imaging sensors. In contrast, optical time stretch technique imaging flow cytometry has previously been demonstrated to enable quantitative phase imaging at an imaging line scan rate >20 MHz with interferometric configuration [26]. With the phase gradient image produced by ATOM, we here can demonstrate another time-stretch imaging modality, Q-ATOM, which is less sensitive to motion artefact and less computationally intensive to generate phase images. This could be an effective instrument for ultra-large scale, high-throughput "single-phytoplankton" analysis with morphological and quantitative information for limnological research and industry.

2. EXPERIMENTS AND RESULTS

The optical system of the new imaging modality, Q-ATOM is similar to the previous one published in [11]. The imaging system mainly consist of two parts – time-stretch and spectral-encoding imaging. A broadband laser pulse (bandwidth = 10 nm, central wavelength = 1064 nm, repetition rate = 11.6 MHz) is first launched into a long optical fiber which transforms the spectrum of the pulse into time domain by optical time-stretching. The pulse then passes through a spatial disperser (e.g. diffraction grating) and form a one dimensional spectral shower. The spectral shower is then focused onto the sample plane which is the middle plane of the microfluidic channel with cells flowing in an orthogonal direction at 2 m/s (corresponding imaging throughput ~100,000 cells/sec). The spatial information of the cell is encoded to the spectrum of the laser pulse line by line (and hence pulse-by-pulse). The line spectrum is then recombined through the same spatial disperser and is finally represented in a serial temporal form which can be captured with a single pixel detector (10 GHz) and an oscilloscope (80 GS/s, 16.8 GHz). This is the previously demonstrated ATOM system in

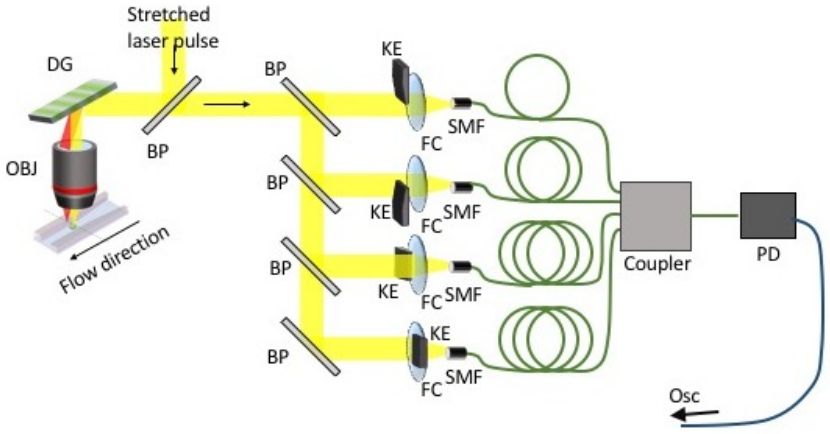

Figure 1. Schematics of Q-ATOM. DG: diffraction grating, OBJ: objective lens, BP: beam splitter, KE: knife-edge, FC: fiber collimator, SMF: single mode fiber, PD: photodiode, Osc: oscilloscope. Knife-edge approach is implemented that the location of the knife edge is in the top, bottom, left and right parts of the Fourier plane before coupling into fiber.

bright-field imaging configuration that produce one image only. For Q-ATOM, the light pulse is split into four paths which corresponds to four different images of the same cell similar in [11] but knife-edge approach is used in the asymmetric detection as shown in Figure. 1. The knife edges are placed in four different positions, and hence provide a partial blockade of the circular light beam before coupling into fiber, such that four Q-ATOM raw images with different contrasts can be generated by this asymmetric fiber-coupling approach (Fig. 2 (a)). This helps generate two pairs of asymmetric images, of which the images of each pair show opposite contrast to each other. The contrast of the images generated is enhanced, making the transparent object observable based on the principle of Schlieren imaging. The four signals are then multiplexed in time domain without overlapping by introducing a small different temporal delay in each path. Therefore, the time-multiplexed signal finally becomes a temporal waveform (total duty ratio < 1) containing four asymmetric images with the same repetition rate and is then detected by the single pixel detector and oscilloscope at the same line scan rate of 11.6 MHz as in [12]. Scenedesmus which is previously used in [12] for demonstrating classification is selected and loaded into the custom-designed microfluidic channel. This species is selected since it is common in many freshwater environments which could be grown either photoautotrophically, heterotrophically, or photoheterotrophically and it is one of the best suitable candidates for biofuel production due to its rich lipid content. Figure. 2(a&b) shows the four selected Q-ATOM images and the corresponding absorption and phase gradient images of a scenedesmus cell.

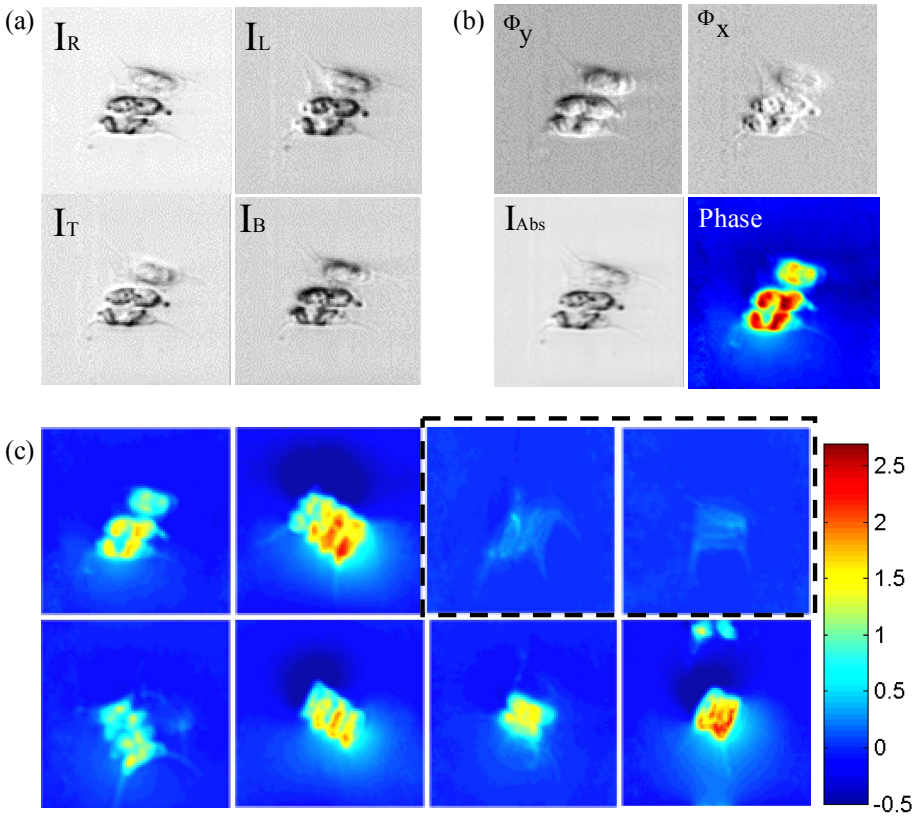

Figure. 2 (a) Four asymmetric images and (b) the corresponding differential-phase gradients (Φ_x, Φ_y), absorption contrast (I_{Abs}) and the reconstructed phase images of selected single scenedesmus. (c) Selected reconstructed phase images of scenedesmus plotted in same color scale. The phase images of dead cells are enclosed in the dashed-line box. The low phase value indicates that the intracellular content has been leaked out in the dead cells. Therefore, only the apparent cell wall is remained.

Similar to the principle in [27,28], wavefront tilt occurs when there is refractive index difference between the sample and the media. It results in a displacement difference increasing or decreasing the intensity of the affected region in the image. Wavefront tilt is first calculated by the equation based on simple geometrical consideration that the phase gradient along horizontal (or vertical) direction is equal to the intensity difference between the opposite horizontal (or vertical) asymmetric image. The influence of the absorption contrast is cancelled when the two images subtract each other and therefore produce an image with differential-phase gradient contrast only (Fig. 2(b)). The relationship between wavefront tilt angle (θ) and phase gradient is therefore given by

$$\vec{\nabla}\phi = 2\pi / \bar{\lambda} \times \vec{\theta}(x,y) \tag{1}$$

where $\bar{\lambda}$ is the central wavelength and ϕ is the local phase shift, in radians, induced by the sample. To generate a comprehensive phase profile of the sample, the phase value is retrieved using the complex Fourier integration method which takes account of the field-of-view (FOV) of the image. This method is specifically chosen due to it robustness and the minimal iterative processes. Figure. 2(c) (color) shows the selected images of the phase image of single scenedesmus captured and reconstructed by Q-ATOM. It should be noted that the phase value of the live pigmented ones is much higher then the hollow (dead) ones in which the intracellular components are leaked out. Besides, it is shown that there is high peak value in certain area where possibly palmitate and oleate (lipid content) accumulate. The spines of the scenedesmus can also be observed in some of the phase images. In spite of the fact that the common biovolume estimation based on simple geometrical model does not consider the complex shape with spine, Q-ATOM has the advantage of calculating the cell volume represent the actual shape with complex structure in a more accurate way.

3. DISCUSSION

The existing methods of classifying and analyzing phytoplankton are flow cytometry based on fluorescence signal, electronic counter, imaging flow cytometry providing taxonomic information. With proper taxonomic identification, the community structure and abundance size information could provide an insight to the geographical and limnological research. With the advantage of high throughput and high sensitivity, optical time-stretch imaging flow cytometry (e.g. Q-ATOM) is an effective research tool for these fields by enabling automated taxonomic classification of phytoplankton based on image analysis with proper machine learning (e.g. support vector machine). It also utilizes the advantages of image-based classification that it could differentiate the sub-species, and do live/dead cell analysis based on the gray-scale morphology, and the subsequent analysis, e.g. the power spectrum features and texture information [12]. By assuming the cells are of simple geometrical structure, cell volume can be estimated based on the images obtained from the optical time-stretch imaging and the traditional imaging flow cytometry similar to the work done in [21]. However, the biovolume and the biomass are subject to significant error due to the variability of the inter-species and intra-species heterogeneity. A simple cylindrical or ellipsoidal model could be far less than enough to accurately estimate the cell volume because phytoplankton cells have more complex shape accommodating structures like filament or spines and have vacuoles which do not have biomass. Therefore, optical quantitative-phase time stretch imaging flow cytometry is an attractive tool to provide a comprehensive analysis on every single phytoplankton without scarifying the throughput as in conventional QPI and manual microscopic inspection. Quantitative phase imaging and analysis is an attractive platform for many biological and biomedical research due to its label-free nature and its comprehensive morphological and quantitative-phase information. In many literatures, QPI could give the information of the cell structure, single cell dry mass, integral refractive index map, two-dimensional angular light scattering information and many other parameters affect cell dynamic and homeostasis of the living cells [25,29]. These pieces of information are particularly intriguing in phytoplankton research. In fact, to monitor the climate change such as the atmospheric CO_2, an ultralarge amount of samples both globally and locally across seasons and years is needed to be analyzed. Proper taxonomic identification and information about the carbon content and other metabolite composition concentration is essential for conducting a comprehensive phytoplankton survey. The information of the organic carbon content inside the algal cells could help understand the carbon cycle dynamics and atmospheric change since phytoplankton is the major producer of carbon and oxygen. Besides, in production of biofuel and other pharmaceutical and cosmetic products, information of the dry mass and the useful substance concentration can help the industry maximally utilize the specific cultured species and hence help culture the cells in a more economical way. Quantitative optical time-stretch imaging flow cytometry is an effective alternative to provide sufficient information of the phytoplankton in large scale for these applications. With the non-inteferometric time-stretch imaging modality, phase image could be generated based on simple mathematics without

iterative processes and be less sensitive to motion artefacts. The measured phase value which represents the wavefront tilting across the sample could also be expressed as optical path-length difference between the cell and the medium, e.g. OPD = n(refractive index) x h(height). The dry mass is then calculated by this equation

$$\iint_S OPD(x,y)\,dx\,dy = \alpha m \tag{2}$$

where S is the projected surface area of the cell, m is the sample dry mass and α is the specific refractive increment which is 0.14-0.15 $cm^3\ g^{-1}$ for carbohydrate and lipids and 0.16-0.2 $cm^3 g^{-1}$ for nucleic acids as stated in [30,31]. Using the empirical relationship of intracellular content (y pg $cell^{-1}$) and cell volume (x μm^3) ,y = a x^b where a and b are constants [13-15, 32], it is possible to estimate the cell carbon, nitrogen and protein contents based on the cell volume calculated by Q-ATOM. It definitely could provide a comprehensive database and analytical method on large scale single "phytoplankton" quantitative analysis.

ACKNOWLEDGEMENTS

This work was partially supported by grant from Research Grant Council of the Hong Kong Special Administration Region, China (Project No. 17207715, 17207714, 17205215, HKU 720112E) Innovation and Technology Support Programme (ITS/090/14) and University Development Fund of HKU.

REFERENCES

[1] Cermeno, P., Maranón, E., Pérez, V., Serret, P., Fernández, E., and Castro, C. G. "Phytoplankton size structure and primary production in a highly dynamic coastal ecosystem (Ría de Vigo, NW-Spain): seasonal and short-time scale variability," Estuarine, Coastal and Shelf Science, 67(1), 251-266.(2006)

[2] Culotta, E. "Red menace in the world's oceans," Science, 257(5076), 1476-1477.(1992)

[3] Manoylov, K. M. "Taxonomic identification of algae (morphological and molecular): species concepts, methodologies, and their implications for ecological bioassessment," Journal of Phycology, 50(3), 409-424. (2014)

[4] Finkel, Z. V., Beardall, J., Flynn, K. J., Quigg, A., Rees, T. A. V., and Raven, J. A. "Phytoplankton in a changing world: cell size and elemental stoichiometry," Journal of Plankton Research, fbp098.(2009)

[5] Boyce, D. G., Lewis, M. R., and Worm, B. "Global phytoplankton decline over the past century," Nature, 466(7306), 591-596. (2010)

[6] Sieracki, C. K., Sieracki, M. E., and Yentsch, C. S. "An imaging-in-flow system for automated analysis of marine microplankton," Marine Ecology Progress Series, 168, 285-296. (1998)

[7] Sosik, H. M., and Olson, R. J. "Automated taxonomic classification of phytoplankton sampled with imaging-in-flow cytometry," Limnology and Oceanography: Methods, 5(6), 204-216. (2007)

[8] Goda, K., Tsia, K. K., and Jalali, B. "Serial time-encoded amplified imaging for real-time observation of fast dynamic phenomena," Nature, 458(7242), 1145-1149. (2009)

[9] Goda, K., Ayazi, A., Gossett, D. R., Sadasivam, J., Lonappan, C. K., Sollier, E., Fard, A. M., Huy, S. C., Adam, J., Murray, C., Wang, C, Brackbill, N., Carlo, D.D., Jalali, B.. "High-throughput single-microparticle imaging flow analyzer," Proc. Natl. Acad. Sci. U. S. A., 109(29), 11630-11635. (2012)

[10] Wong, T. T., Lau, A. K., Wong, K. K., and Tsia, K. K. "Optical time-stretch confocal microscopy at 1 μm," Optics Letters, 37(16), 3330-3332. (2012)

[11] Wong, T. T., Lau, A. K., Ho, K. K., Tang, M. Y., Robles, J. D., Wei, X., Chan, A. C., Tang, A. H., Lam, E. Y., Wong, K. Y., Chan, G. C., Shum, H. C. and Tsia, K. K. "Asymmetric-detection time-stretch optical microscopy (ATOM) for ultrafast high-contrast cellular imaging in flow," Scientific Reports, 4. (2014)

[12] Lai, Q. T., Lau, A. K., Wong, K. K. and Tsia, K. K. "Optical time-stretch imaging flow cytometry of phytoplankton," 2105 International Photonic conference (2015)

[13] Mullin, M. M., Sloan, P. R., and Eppley, R. W. "Relationship between carbon content, cell volume, and area in phytoplankton," Limnology and Oceanography, 11(2), 307-311. (1966)

[14] Aas, E. "Refractive index of phytoplankton derived from its metabolite composition," Journal of Plankton Research, 18(12), 2223-2249. (1996)

[15] Stramski, D. "Refractive index of planktonic cells as a measure of cellular carbon and chlorophyll a content," Deep Sea Research Part I: Oceanographic Research Papers, 46(2), 335-351. (1999)

[16] Mata, T. M., Martins, A. A., and Caetano, N. S. "Microalgae for biodiesel production and other applications: a review," Renewable and sustainable energy reviews, 14(1), 217-232. (2010)
[17] Billington, N. "A comparison of three methods of measuring phytoplankton biomass on a daily and seasonal basis," Hydrobiologia, 226(1), 1-15. (1991)
[18] Sun, J., and Liu, D. "Geometric models for calculating cell biovolume and surface area for phytoplankton," Journal of Plankton Research, 25(11), 1331-1346. (2003)
[19] Hallegraeff, G. M. "A comparison of different methods used for the quantitative evaluation of biomass of freshwater phytoplankton," Hydrobiologia, *55*(2), 145-165. (1977)
[20] Beattie, D. M., Golterman, H. L., and Vijverberg, J. "An introduction to the limnology of the Friesian lakes," Hydrobiologia, 58(1), 49-64. (1978)
[21] Álvarez, E., López-Urrutia, Á., and Nogueira, E. "Improvement of plankton biovolume estimates derived from image-based automatic sampling devices: application to FlowCAM," Journal of Plankton Research, 34(6), 454-469. (2012)
[22] Rappaz, B., Cano, E., Colomb, T., Kühn, J., Depeursinge, C., Simanis, V., Magistretti, P. J. and Marquet, P. "Noninvasive characterization of the fission yeast cell cycle by monitoring dry mass with digital holographic microscopy," Journal of biomedical optics, 14(3), 034049-034049. (2009).
[23] Ikeda, T., Popescu, G., Dasari, R. R., and Feld, M. S. "Hilbert phase microscopy for investigating fast dynamics in transparent systems," Optics letters, 30(10), 1165-1167. (2005).
[24] Sung, Y., Tzur, A., Oh, S., Choi, W., Li, V., Dasari, R. R., Yaqoob, Z. and Kirschner, M. W. "Size homeostasis in adherent cells studied by synthetic phase microscopy," Proc. Natl. Acad. Sci. U. S. A. 110(41),16687–16692 (2013)
[25] Lee, K., Kim, K., Jung, J., Heo, J., Cho, S., Lee, S., Chang, G., Jo, Y, Park, h. and Park, Y. "Quantitative phase imaging techniques for the study of cell pathophysiology: from principles to applications," Sensors, 13(4), 4170-4191. (2013)
[26] Lau, A. K., Wong, T. T., Ho, K. K., Tang, M. T., Chan, A. C., Wei, X., Lam, E. Y., Shum, H. C., Wong, K. Y and Tsia, K. K. "Interferometric time-stretch microscopy for ultrafast quantitative cellular and tissue imaging at 1 μm," Journal of Biomedical Optics, 19(7), 076001-076001 (2014)
[27] Parthasarathy, A. B., Chu, K. K., Ford, T. N., and Mertz, J. "Quantitative phase imaging using a partitioned detection aperture," Optics Letters, 37(19), 4062-4064. (2012)
[28] Iglesias, I. "Pyramid phase microscopy," Optics Letters, 36(18), 3636-3638. (2011)
[29] Aknoun, S., Savatier, J., Bon, P., Galland, F., Abdeladim, L., Wattellier, B., and Monneret, S. "Living cell dry mass measurement using quantitative phase imaging with quadriwave lateral shearing interferometry: an accuracy and sensitivity discussion." Journal of Biomedical Optics, 20(12), 126009-126009. (2015)
[30] Barer, R., and Joseph, S. "Refractometry of living cells part I. Basic principles." Quarterly Journal of Microscopical Science, 3(32), 399-423. (1954)
[31] Barer, R., Ross, K. F., and Tkaczyk, S. "Refractometry of living cells." Nature, 171(4356), 720. (1953)
[32] Montagnes, D. J., Berges, J. A., Harrison, P. J., and Taylor, F." Estimating carbon, nitrogen, protein, and chlorophyll a from volume in marine phytoplankton." Limnology and Oceanography, 39(5), 1044-1060. (1994)